High-Frequency EPR and Pulsed Q-Band ENDOR Studies on the Origin of the Hydrogen Bond in Tyrosyl Radicals of Ribonucleotide Reductase R2 Proteins from Mouse and Herpes Simplex Virus Type 1

Pieter J. van Dam,[†] Jean-Paul Willems,[‡] Peter P. Schmidt,[§] Stephan Pötsch,[⊥] Anne-Laure Barra,[||] Wilfred R. Hagen,*[,†] Brian M. Hoffman,*[,‡] K. Kristoffer Andersson,*[,§] and Astrid Gräslund*[,⊥]

Contribution from the Department of Molecular Spectroscopy, University of Nijmegen, Toernooiveld 1, 6525 ED Nijmegen, The Netherlands, Department of Chemistry, Northwestern University, 2145 Sheridan Road, Evanston, Illinois 60208-3113, Department of Biochemistry, University of Oslo, P.O. Box 1041 Blindern, N-0316 Oslo, Norway, Department of Biophysics, Stockholm University, S-106 91 Stockholm, Sweden, and High Magnetic Field Laboratory, CNRS, B.P. 166, F-38042 Grenoble Cedex 9, France

Received October 27, 1997

Abstract: The **g** tensor of the tyrosyl radical present in the active R2 protein of ribonucleotide reductase is anisotropic, and the g_1 component is influenced by hydrogen bonding to the oxygen of the tyrosyl ring. We have studied the tyrosyl radical in the R2 protein of *Escherichia coli*, mouse, and herpes simplex virus type 1 (HSV1) with high-frequency EPR and pulsed ENDOR after reconstitution in D_2O. From the high-frequency EPR measurements the **g** tensor of the radical in HSV1 RNR R2 was found to be identical to that in mouse R2, indicating the presence of a hydrogen bond to the phenolic oxygen in both cases, and in contrast to that in *E. coli* R2. The pulsed ENDOR spectra confirmed the absence of an exchangeable proton near the tyrosyl radical in *E. coli* R2. For mouse and HSV1 R2 a clear ENDOR signal of exchanged deuterium was found with a hyperfine splitting of −0.53 MHz (mouse) and −0.56 MHz (HSV1). This was interpreted as a proton at a distance of 1.89 Å (mouse) and 1.86 Å (HSV1) from the phenolic oxygen with an orientation, derived from simulations, in the plane of the tyrosyl ring. The most likely origin of this proton is the water ligand at Fe1. This is in contrast with photosystem II where the hydrogen bonding to the radical $Y_D^{\bullet}$ was formed by a nearby histidine. The presence of the hydrogen bond to the tyrosyl radical may be related to the faster spin−lattice relaxation for the mouse and HSV1 radical compared to that for the *E. coli* radical, as measured before by Galli et al. [*J. Am. Chem. Soc.* **1995**, *117*, 740−746]. It seems therefore likely that the distance between the tyrosyl radical and the iron−oxygen cluster in mouse and HSV1 R2 proteins is shorter compared to that in *E. coli* R2. Since the tyrosyl radicals in the HSV1 and mouse R2 proteins are much more accessible to the solvent, the hydrogen bond may play a useful role in stabilizing the tyrosyl radical.

Introduction

The highly regulated enzyme ribonucleotide reductase (RNR) catalyzes the reduction of ribonucleotides to deoxyribonucleotides which are precursors in the synthesis of DNA in all living organisms.[1] Several classes of RNR have been described with different cofactors,[2−6] which are all needed as a source of free radicals which can generate a postulated thiyl radical in the active site.[2,7,8] These thiyl radicals are able to initiate catalysis by abstracting the H3-hydrogen from the ribose moiety of the different ribonucleotides (for recent reviews on general mechanisms of the aerobic and anaerobic classes of RNR and different radical-generating systems see refs 1−8). Class I RNR enzymes as described in this work contain a stable tyrosyl radical of a neutral phenolic type and a diferric iron−oxygen center in the catalytically active form of the smaller subunit protein R2. Free radicals on tyrosyl residues have been found in RNR from several different sources, as well as in photosystem II (PSII) and prostaglandin H synthase.[9−11]

Class I RNR consists of a 1:1 complex of two proteins, R1 and R2, each of which is a homodimer. The crystal structures of *Escherichia coli* proteins R1 and R2 have been determined.[12−14] Model building studies of the R1:R2 complex suggest that the radical/iron site in the *E. coli* RNR R2 is about 35 Å from the

* Corresponding authors.
[†] University of Nijmegen.
[‡] Northwestern University.
[§] University of Oslo.
[⊥] Stockholm University.
[||] CNRS.

(1) Reichard, P. *Science* **1993**, *260*, 1773−1777.
(2) Stubbe, J.; van der Donk, W. *Chem. Biol.* **1995**, *2*, 793−801.
(3) Sjöberg, B. M. *Nucleic Acids Mol. Biol.* **1995**, *9*, 192−221.
(4) Gräslund, A.; Sahlin, M. *Annu. Rev. Biophys. Biomol. Struct.* **1996**, *25*, 259−286.
(5) Andersson, K. K.; Gräslund, A. *Adv. Inorg. Chem.* **1995**, *43*, 359−409.
(6) Fontecave, M.; Nordlund, P.; Eklund, H.; Reichard, P. *Adv. Enzymol.* **1992**, *65*, 147−183.
(7) Stubbe, J. *Adv. Enzymol.* **1990**, *63*, 349−419.
(8) Licht, S.; Gerfen, G. J.; Stubbe, J. *Science* **1996**, *271*, 477−481.
(9) Barry, B. A.; Babcock, G. T. *Proc. Natl. Acad. Sci. U.S.A.* **1987**, *84*, 7099−7103.
(10) Babcock, G. T.; Barry, B. A.; Debus, R. J.; Hoganson, C. W.; Atamian, M.; McIntosh, L.; Sithole, I.; Yocum, C. F. *Biochemistry* **1989**, *28*, 9557−9565.
(11) Prince, R. C. *Trends Biochem. Sci.* **1988**, *13*, 286−288.
(12) Uhlin, U.; Eklund, H. *Nature* **1994**, *370*, 533−539.
(13) Nordlund, P.; Sjöberg, B.-M.; Eklund, H. *Nature* **1990**, *345*, 593−598.

S0002-7863(97)03712-8 CCC: $15.00
Published on Web 05/07/1998

substrate binding active site in protein R1.[12] Therefore, a long proton (H^0 radical) transfer path between the two sites is needed. The tyrosine residue that will become the stable deprotonated tyrosyl radical, which is necessary for normal enzymatic activity, is found at a distance of 5 Å from the closest iron (Fe1) of the iron−oxygen cluster in the *E. coli* R2 protein in the so-called met-state without radical. The three-dimensional structure of active radical containing R2 protein is not known. The fate of the phenolic hydrogen on the tyrosine, which is lost when the tyrosyl radical is formed in RNR R2, may be of importance for understanding the long-range electron/proton transfer that is postulated to occur in the enzymatic reaction and in the generation of the radical.[15−21]

The crystal structure of the mouse R2 protein has been resolved recently;[14] however, the iron−oxygen cluster was lacking one of the iron atoms. No three-dimensional structures of any of the herpes simplex virus type 1 (HSV1) RNR proteins are known.

Tyrosyl radicals in the class I RNR exhibit differences in dihedral angles of the tyrosyl β-methylene protons.[22,23] Also, high-frequency EPR studies showed differences in the **g** value anisotropy between different species.[24] The radicals from *E. coli* and *Salmonella typhimurium* RNR have a relatively large **g** anisotropy with the low-field tensor component ($g_1 = 2.009$) directed along the C−O bond of the tyrosyl ring.[25] The tyrosyl radical in mouse RNR had a lower g_1 value of 2.0076,[24] similar to that observed for the dark stable tyrosyl radical ($Y_D^{\bullet}$) in PSII.[26,27] On the basis of a comparison with $Y_D^{\bullet}$ and model complexes, this difference in g_1 value between *E. coli* R2 and mouse R2 has been interpreted for the mouse R2 radical and the $Y_D^{\bullet}$ radical as the result of a hydrogen bond with a nearby hydrogen. This hydrogen bond is absent in *E. coli* and *S. typhimurium* RNR. This was confirmed in ESEEM and ENDOR studies of the *E. coli* RNR R2 radical, which failed to detect any solvent exchangeable proton close to the radical.[28]

To further catalog these different proteins, we have extended the series of high-frequency EPR measurements on RNR R2 to HSV1. In addition to these measurements we have done 35 GHz pulsed ENDOR experiments in order to determine the distance(s) and orientation(s) of the solvent exchangeable proton(s) with respect to the tyrosyl ring in the RNR R2 protein from mouse, herpes, and *E. coli* RNR R2. In this study we demonstrate for the first time the presence of a water exchangeable proton that forms a hydrogen bridge to the tyrosyl radical in the mouse and HSV1 R2 proteins and which is absent in the *E. coli* R2 protein.

Materials and Methods

Sample Preparation. Recombinant mouse and HSV1 R2 proteins were prepared as previously reported.[29] Active mouse and HSV1 proteins were produced from iron-free apoproteins by reconstitution in 50 mM Tris−HCl, pH 7.6, 100 mM KCl with ferrous iron and oxygen as previously described,[30,31] using six Fe(II) atoms per RNR R2. Exchange of apoprotein and reconstitution in 99.5% D_2O was done using deuterated buffer corrected for deuterium effects and with centrifuge columns of Sephadex G25, described before.[30,31] After reconstitution in H_2O or D_2O buffer (corrected for deuterium effects) the samples were transferred into 50 mM Tris−HCl or 100 mM Tris−DCl at pH 7.6, 100 mM KCl in H_2O or D_2O, using a Sephadex G25 centrifuge column, thereby removing excess iron. Finally glycerol was slowly added to a final concentration of 20% (v/v). The *E. coli* RNR R2 was used as isolated in active form[32] in 50 mM Tris−HCl pH 7.5 and 100 mM KCl. The deuterated *E. coli* R2 sample was exchanged into D_2O, but not reconstituted in D_2O, using deuterated buffer with centrifuge columns as for the mouse and HSV1 R2 proteins. The iron and radical contents of the samples were as previously reported[29,31,32] judged from light absorption spectra and EPR characteristics. All samples were checked by X-band EPR in the range 25−77 K and showed previously reported behavior.[30] For the *E. coli* and mouse samples the radical:protein ratio was above 1 (theoretical maximum 2), while the HSV1 radical content was 0.3 per protein R2.

High-Frequency EPR. For the 130 GHz experiments a spectrometer previously described was used.[33] The high-frequency EPR spectra of the tyrosyl radical are recorded as dispersion signals in phase with the field modulation.[34] This is the result of the experimental conditions: a high $\mathbf{B}_1$ field at these shorter wavelengths in combination with a high modulation frequency (20 kHz) and a spin−lattice relaxation at 5 K of $T_1 = 50$ ms.[30] The condition $\omega T_1 \gg 1$, required for rapid passage effects,[35] is fulfilled, leading to the shape of a negative, unmodulated absorption signal.[36] Numerical differentiation was used to present the spectra in the common derivative line shape of EPR spectra.

The 245 GHz EPR spectrometer is a home-built multifrequency spectrometer, measuring simply the transmission of the exciting light through the sample. The main frequency source is an optically pumped far infrared laser. The 245 GHz line ($\lambda = 1223.67$ μm) is obtained using methanol gas for the far-IR laser. A small modulation field is superimposed to the main field so that the derivative of the transmission is recorded. An InSb bolometer (QMC Instruments) is used for the detection, enabling the small field to be modulated at 10 kHz. The main magnetic field is provided by a superconducting magnet (Cryogenics Consultant), which generates fields up to 12 T.[24,25,37,38]

(14) Kauppi, B.; Nielsen, B. B.; Ramaswarmy, S.; Larsen, I. K.; Thelander, M.; Thelander, L.; Eklund, H. *J. Mol. Biol.* **1996**, *262*, 706−720.
(15) Bollinger, J. M.; Edmondson, D. E.; Huynh, B.-H.; Filley, J.; Norton, J. R.; Stubbe, J. *Science* **1991**, *253*, 292−298.
(16) Bollinger, J. M.; Tong, W. H.; Ravi, N.; Huynh, B.-H.; Edmondson, D. E.; Stubbe, J. *J. Am. Chem. Soc.* **1994**, *116*, 8015−8023.
(17) Bollinger, J. M.; Tong, W. H.; Ravi, N.; Huynh, B.-H.; Edmondson, D. E.; Stubbe, J. *J. Am. Chem. Soc.* **1994**, *116*, 8024−8032.
(18) Sahlin, M.; Lassmann, G.; Pötsch, S.; Sjöberg, B.-M.; Gräslund, A. *J. Biol. Chem.* **1995**, *270*, 12361−12372.
(19) Rova, U.; Goodtzova, K.; Ingemarson, R.; Behravan, G.; Gräslund, A.; Thelander, L. *Biochemistry* **1995**, *34*, 4267−4275.
(20) Burdi, D.; Sturgeon, B. E.; Tong, W. H.; Stubbe, J.; Hoffman, B. *J. Am. Chem. Soc.* **1996**, *118*, 281−282.
(21) Siegbahn, P. E. M.; Blomberg, M. R. A.; Crabtree, R. H. *Theor. Chem. Acc.* **1997**, *97*, 289−300.
(22) Jordan, A.; Pontis, E.; Atta, M.; Krook, M.; Gibert, I.; Barbe, J.; Reichard, P. *Proc. Natl. Acad. Sci.* U.S.A. **1994**, *91*, 12892−12896.
(23) Himo, F.; Gräslund, A.; Eriksson, L. A. *Biophys. J.* **1997**, *72*, 1556−1567.
(24) Schmidt, P. P.; Andersson, K.; Barra, A.-L.; Thelander, L.; Gräslund, A. *J. Biol.* Chem. **1996**, *271*, 23615−23618.
(25) Allard, P.; Barra, A.; Andersson, K.; Schmidt, P.; Atta, M.; Gräslund, A. *J. Am. Chem. Soc.* **1996**, *118*, 895−896.
(26) Un, S.; Brunel, L.-C.; Brill, T. M.; Zimmerman, J.-L.; Rutherford, A. W. *Proc. Natl. Acad. Sci. U.S.A.* **1994**, *91*, 5262−5266.
(27) Un, S.; Atta, M.; Fontecave, M.; Rutherford, A. W. *J. Am. Chem. Soc.* **1995**, *117*, 10713−10719.
(28) Hoganson, C. W.; Sahlin, M.; Sjöberg, B.-M.; Babcock, G. T. *J. Am. Chem. Soc.* **1996**, *118*, 4672−4679.
(29) Mann, G. J.; Gräslund, A.; Ochiai, E.-I.; Ingemarson, R.; Thelander, L. *Biochemistry* **1991**, *30*, 1939−1947.
(30) Galli, C.; Atta, M.; Andersson, K. K.; Gräslund, A.; Brudvig, G. W. *J. Am. Chem. Soc.* **1995**, *117*, 740−746.
(31) Atta, M.; Debaecker, N.; Andersson, K. K.; Latour, J.-M.; Thelander, L.; Gräslund, A. *J. Biol. Inorg. Chem.* **1996**, *1*, 210−220.
(32) Sjöberg, B.-M.; Hahne, S.; Karlsson, M.; Jörnvall, H.; Göransson, M.; Uhlin, B. E. *J. Biol. Chem.* **1986**, *261*, 5658−5662.
(33) van Dam, P. J.; Klaassen, A. A. K.; Reijerse, E. J.; Hagen, W. R. *J. Magn. Reson.* **1998**, *130*, 140−144.
(34) Farrer, C. T.; Gerfen, G. J.; griffen, R. G.; Force, D. A.; Britt, R. D. *J. Phys. Chem. B* **1997**, *101*, 6634−6641.
(35) Mailer, C.; Taylor, C. P. S. *Biochim. Biophys. Acta* **1973**, *322*, 195−203.
(36) Ammerlaan, C. A. J.; van der Wiel, A. *J. Magn. Reson.* **1976**, *21*, 387−396.
(37) Muller, F.; Hopkins, M. A.; Coron, N.; Grynberg, M.; Brunel, L. C.; Martinez, G. *Rev. Sci. Instrum.* **1989**, *60*, 3681−3684.
(38) Barra, A. L.; Brunel, L. C.; Robert, J. B. *Chem. Phys. Lett.* **1990**, *165*, 107−109.

ENDOR Spectroscopy. A description of the 35 GHz pulsed ENDOR spectrometer employed in this study has been published recently.[39] Deuterium ENDOR spectra were collected using the Mims stimulated-echo ENDOR pulse sequence ($(\pi/2)-\tau-(\pi/2)-$RF pulse$-(\pi/2)-\tau-$echo).[40,41] Pulsed ENDOR spectra measured with this sequence are hampered by the so-called dead-spots depending on the pulse interval τ and the hyperfine coupling A. The ENDOR response, R, depends on both these quantities according to

$$R \propto 1 - \cos(2\pi A\tau) \qquad (1)$$

Undistorted line shapes that are essential for accurate simulations can only be expected in the case that $A\tau < 1/2$.[42] The minimum value of τ that can be used is determined by the sample/resonator combination. In our pulsed ENDOR measurements a τ value of 480 ns was used, implying that the maximal undistorted hyperfine coupling is 1.05 MHz, equal to an exchanged proton with a coupling of 6.8 MHz. The deuterium ENDOR signal obtained in this way consists of a doublet centered at υ_D and split by A_D, with an additional splitting caused by the nuclear quadrupole interaction. To facilitate a comparison, the 35 GHz pulsed ENDOR deuterium spectra have been centered around the deuterium Larmor frequency.

The weakly anisotropic **g** tensor of a tyrosyl radical gives very poor orientation selection even at 35 GHz, but analysis of the ^{2}H hyperfine and quadrupole tensors could nonetheless be performed by collecting spectra across the EPR envelope and analyzing according to procedures described before.[43−45] ENDOR simulations were performed on a PC using the program Gensim, a modified version of the simulation program GENDOR, which speeds calculations when orientation selectivity is poor as in this case.

Results

The high-frequency EPR spectrum of the tyrosyl radical in RNR R2 from herpes simplex virus 1 was measured at 245 GHz. The spectrum is presented in Figure 1 together with a previously recorded spectrum of the tyrosyl radical from mouse RNR R2.[24] The two species proved to have similar EPR spectra with an identical **g** tensor, the principal components of which are $g_1 = 2.0076$, $g_2 = 2.0043$, and $g_3 = 2.0022$. The 245 GHz spectrum of HSV1 R2 could be simulated with approximately the same parameters as for the mouse protein (simulation not shown).[46] The inset in Figure 1 shows 130 GHz EPR spectra of the samples of all three species of RNR R2 used in this study. Clearly the lowering of the g_1 value in the spectrum of mouse and HSV1 RNR R2 protein compared to *E. coli* RNR R2 is visible. The g_1 values were checked by using a background signal of Mn^{2+} using the method as described by Burghaus et al.[47] Due to rapid passage effects and field inhomogeneity of the Bitter magnet, the strong splitting caused by one of the β-methylene protons is not visible in these 130 GHz spectra.

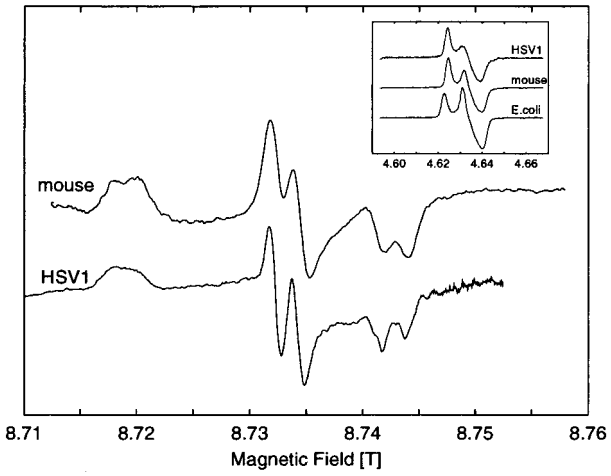

Figure 1. The 245 GHz spectra of the mouse (0.75 mM, from Schmidt et al.[24]) and HSV1 R2 tyrosyl radical (0.25 mM): microwave frequency, 244.997 GHz; field modulation, 3.5 G; modulation frequency, 10 kHz; temperature, 5 K. The inset shows the 130 GHz EPR spectra of the tyrosyl radical in RNR R2 from *E. coli* 0.57 mM (bottom), mouse (middle), and HSV1 0.25 mM (top). Due to the hydrogen bond the g_1 value is reduced compared to R2 from *E. coli*. Conditions: microwave frequency, 129.97 GHz; modulation frequency, 20 kHz; modulation amplitude, 2 G; temperature, 5 K.

Table 1. g_1 Values for Tyrosyl Radicals in RNR Measured by High-Frequency EPR Spectroscopy Compared to Previously Reported g_1 Values of Tyrosyl Radicals

species	g_1 value	ref
E. coli R2	2.0091	this work
	2.00868	Un et al.[48]
mouse R2	2.0076	Schmidt et al.[24]
herpes (HSV1) R2	2.0076	this work
typhimurium R2	2.0089	Allard et al.[25]
$Y_D^\bullet$ in spinach PSII	2.00745	Un et al.[27]
$Y_D^\bullet$ in spinach PSII	2.0075	Un et al.[48]
γ-irradiated tyrosine	2.0067	Fasanella et al.[49]

The g_1 components derived from these measurements are presented in Table 1. For comparison, the previously determined g_1 values of the tyrosyl radical in RNR R2 from *E. coli*,[27] *S. typhimurium*,[25] and mouse[24] are included together with the g_1 values of the tyrosyl radicals $Y_D^\bullet$ and $Y_Z^\bullet$ in photosystem II[26,48,27] and the hydrochloric tyrosine radical.[49] The g_2 and g_3 values of all the tyrosyl radicals studied so far are independent of the surroundings. Three (mouse, photosystem II, and the hydrochloric tyrosine radical) of the five species investigated previously have a relatively low g_1 value. This has been explained with a lower spin density on the phenolic oxygen due to the presence of a hydrogen bond.[27,24,48] Probably, this is also the case for HSV1 RNR R2. Recently, it has been shown[50] that in $Y_D^\bullet$ a nearby histidine (His189) forms the hydrogen bond.

As was suggested by Un et al.[27] the geometrical information that can be obtained about this hydrogen bond is limited when using EPR solely. More detailed information about this hydrogen bond and the orientation of the hydrogen atom with respect to the tyrosyl radical can be obtained with ENDOR spectroscopy. For this purpose the samples were reconstituted in D_2O and studied with Q-band pulsed ENDOR in order to measure signals from the exchangeable protons.

(39) Davoust, C. E.; Doan, P. E.; Hoffman, B. *J. Magn. Reson., A* **1996**, *119*, 38−44.
(40) Mims, W. B. *Proc. R. Soc. London* **1965**, *283*, 452−457.
(41) Gemperle, C.; Schweiger, A. *Chem. Rev.* **1991**, *91*, 1481−1505.
(42) Willems, J.-P.; Lee, H.-I.; Burdi, D.; Doan, P. E.; Stubbe, J.; Hoffman, B. M. *J. Am. Chem. Soc.* **1997**, *119*, 9816−9824.
(43) Hoffman, B. M. *Acc. Chem. Res*. **1991**, *24*, 164−170.
(44) DeRose, V. J.; Hoffman, B. M. *Methods Enzymol*. **1995**, *246*, 554−589.
(45) Hoffman, B. M.; DeRose, V. J.; Doan, P. E.; Gurbiel, R. J.; Houseman, A. L. P.; Telser, J. V. EMR of Paramagnetic Molecules. In *Biological Magnetic Resonance*; Berliner, L. J., Reuben, J., Eds.; Plenum Press: New York, 1993; Vol. 13, pp 151−218.
(46) The complete simulation parameters are ($H^\beta(1)$) $A_{xx} = 64$ MHz, $A_{yy} = 58$ MHz, $A_{zz} = 50$ MHz; ($H^\beta(2)$) $A_{xx} = 11$ MHz, $A_{yy} = 7$ MHz, $A_{zz} = 8$ MHz; ($H^{3,5}(1)$) $A_{xx} = -8$ MHz, $A_{xy} = -8$ MHz, $A_{yy} = -13$ MHz, $A_{zz} = -22$ MHz; and ($H^{3,5}(2)$) $A_{xx} = -12$ MHz, $A_{xy} = 5$ MHz, $A_{yy} = -5$ MHz, $A_{zz} = -18$ MHz. The line width used in the simulations was 9.5 MHz.
(47) Burghaus, O.; Rohrer, M.; Götzinger, T.; Möbius, K. *Meas. Sci. Technol*. **1992**, *3*, 765−774.
(48) Un, S.; Tang, X.; Diner, B. A. *Biochemistry* **1996**, *35*, 679−684.
(49) Fasanella, E. L.; Gordy, W. *Proc. Natl. Acad. Sci. U.S.A.* **1969**, *62*, 299−304.
(50) Campbell, K. A.; Peloquin, J. M.; Diner, B. A.; Tang, X.-S.; Chisholm, D. A.; Britt, R. D. *J. Am. Chem. Soc.* **1997**, *119*, 4787−4788.

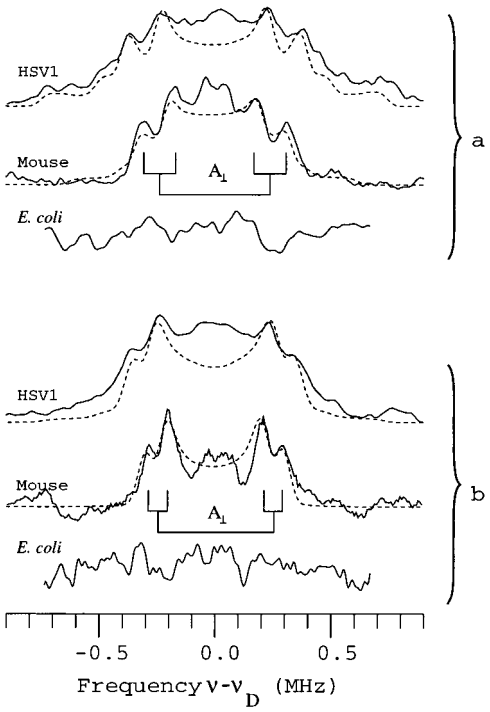

Figure 2. The 35 GHz pulsed Mims ENDOR spectra of RNR R2 in D_2O buffer solution: solid lines, experimental spectra; dashed lines: simulated spectra. The parameters for the simulations are listed in Table 2. The protein was obtained from three different sources: HSV1, mouse, and *E. coli* protein. (a) Spectra taken at a magnetic field position corresponding to the maximum echo intensity. (b) Spectra taken at the high-field edge of the EPR envelope. All spectra have been centered around the nuclear deuterium Larmor frequency. Conditions: RF pulse width, 60 μs; $\tau = 480$ ns; microwave pulse width, 48 ns; temperature, 2 K.

Figure 2 shows the 35 GHz Mims pulsed deuterium ENDOR spectra of HSV1, mouse, and *E. coli* RNR R2 in D_2O buffer, at two of the several field values where spectra were collected: one field value corresponds to the maximum echo intensity, the other corresponds to the high-field "edge" of the EPR envelope. No deuterium signal could be found for the *E. coli* protein anywhere on the EPR envelope, indicating that there is no exchangeable proton near the tyrosyl radical. This suggests that the pocket around the *E. coli* tyrosyl radical is inaccessible to solvent protons. This is in contrast with recent measurements by Force et al.[51] where a deuterium matrix signal was observed in R2 from *E. coli*. Also in that study they did not observe any coordinated deuterium for *E. coli* R2. However, they exchanged their samples much longer (5 h) in D_2O, suggesting that the exchange is much slower in *E. coli* R2 compared to that in the mouse and HSV1 R2 proteins.

In contrast to the *E. coli* spectra, the pulsed ENDOR spectra of the HSV1 and the mouse protein are dominated by a doublet of doublets which is characteristic of the interaction with a single deuterium atom; this is particularly clear for the spectra of the mouse enzyme in Figure 2b. These features are the "perpendicular" singularities of an axial hyperfine tensor with a primary doublet splitting of $A_\perp(D) = -0.53$ MHz for mouse and $A_\perp(D) = -0.56$ MHz for HSV1 (corresponding to a proton hyperfine coupling of -3.45 MHz for mouse and -3.65 MHz for HSV1), with further splitting as a result of the deuterium quadrupole coupling. For both HSV1 and mouse R2 proteins these signals are assigned to a deuteron bonded to the tyrosyl oxygen atom.

(51) Force, D.-A.; Randall, D. W.; Britt, R. D. *Biochemistry* **1997**, *36*, 12062−12070.

Table 2. Simulation Parameters of the Deuterium ENDOR Spectra of the Mouse RNR R2 and HSV1 RNR R2 Spectra As Shown in Figure 2[a]

	mouse	herpes
A_1 (MHz)	1.06	1.12
A_2 (MHz)	−0.53	−0.56
A_3 (MHz)	−0.53	−0.56
P_1 (MHz)	0.07	0.07
P_2 (MHz)	−0.05	−0.05
P_3 (MHz)	−0.02	−0.02
ρ_O	0.3	0.3
r (Å)	1.89	1.86

[a] The EPR line width (FWHM, Gaussian) used was 60 MHz; the ENDOR line width (FWHM, Gaussian) was 0.08 MHz. The **g** values needed for the simulations were taken from Schmidt et al.[24] Euler angles relating the **g** tensor and the **A** tensor used for the simulation of the mouse spectra: $\phi = 0°$, $\theta = 20°$, and $\varphi = 0°$. The hyperfine and quadrupole tensors are taken to be coaxial. HSV1: $\phi = 0°$, $\theta = 20°$, $\varphi = 40°$ also with coinciding hyperfine and quadrupole tensors. These orientations are depicted in Figure 3.

At the magnetic field position corresponding to the maximum echo intensity (Figure 2a), both ENDOR spectra of the HSV1 and mouse protein also show appreciable intensity of the matrix deuterons at the Larmor frequency of deuterium. These "matrix" signals are attributed to nearby, but not hydrogen-bonded, deuterium nuclei.

The spectrum at the echo maximum (Figure 2a) for the HSV1 enzyme shows broad "wings" with edges at 0.7 MHz, which arise from molecules for which the external field lies roughly along the direction of the largest hyperfine interaction. The absence of this feature at the corresponding field for the mouse deuteron signal implies that the hyperfine and quadrupole tensors in the two R2 proteins have different orientations with respect to the **g** tensor. The full sets of spectra collected across the EPR envelopes of the two enzymes were analyzed to obtain the hyperfine and quadrupole tensors that are presented in Table 2. The hyperfine tensors for both the HSV1 and the mouse enzymes are purely dipolar as expected for a hydrogen bond to a tyrosyl residue.[52] In this case the unique axis of the hyperfine tensor points along the O−H/D bond. If we assume the **g** tensor to be oriented as described by Hoganson et al.[28] and Un et al.[27] (i.e., the g_1 component is directed along the carbon−oxygen bond and the g_3 component lies perpendicular to the plane of the tyrosyl ring), then the orientation of this unique axis relative to the tyrosyl ring for the two enzymes is as presented in Figure 3. In the mouse protein the O−H bond lies in the g_1-g_3 plane, which is normal to the ring and passing through the C4−C1−O axis, and is rotated ∼20° out of the tyrosyl plane. In the HSV1 protein the O−H bond is similarly out of plane and is rotated away from the C−O bond by ∼40°. The quadrupole tensors for both enzymes have the same principal values but different orientations. The largest quadrupole component is slightly smaller than that reported by Force et al. for PSII,[52] 0.07 MHz versus 0.1 MHz.

The hyperfine tensor components for the HSV1 enzyme are similar to those reported for $Y_D^\bullet$ in PSII[52] while the hyperfine tensor values for mouse RNR are slightly smaller. From the dipolar hyperfine coupling the distance between the H-bonded proton/deuteron and the oxygen of the tyrosyl ring can be calculated using the following equation:

$$A_{dip} = \rho_O g_e g_N \beta_e \beta_N / r^3 \qquad (2)$$

where ρ_O is the unpaired spin density on the tyrosyl oxygen, g_e

(52) Force, D.-A.; Randall, D. W.; Britt, R. D.; Tang, X.-S.; Diner, B. A. *J. Am. Chem. Soc.* **1995**, *117*, 12643−12644.

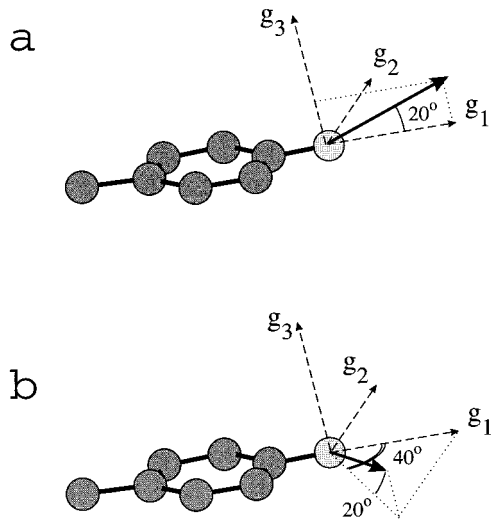

Figure 3. Orientation of the maximum hyperfine tensor component (A^{max}) with respect to the molecular frame. The **g** tensor has been indicated by the dashed arrows; A^{max} is depicted by the solid arrow. The oxygen atom is represented by the light gray circle. The accuracy of the numerical values of the angles is 10°. (a) Mouse tyrosyl RNR R2. (b) HSV1 tyrosyl RNR R2.

the electron g factor, g_N the nuclear g factor, β_e the electron Bohr magneton, and β_N the nuclear Bohr magneton. The hydrogen bond distance that can be calculated with this equation depends on the determined phenolic oxygen spin density (ρ_O). Theoretical calculations based on density functional theory indicate that an isolated tyrosyl radical should have an unpaired spin density on the oxygen atom of 0.37 and that this value may be reduced by about 0.05 in the presence of a hydrogen bond.[23] Other calculations by Farrar et al.[34] showed less reduction of the spin density of the phenolic oxygen of about 0.024 for a hydrogen bond of 1.7 Å. Recent experimental results on tyrosyl radicals in frozen aqueous solution, *E. coli* protein R2, and $Y_D^\bullet$ of photosystem II yielded phenolic oxygen spin density values of 0.26, 0.29, and 0.28, respectively,[28,53,54] determined from ^{17}O hyperfine couplings using empirical values for the McConnell rules. Although the hyperfine couplings are determined with good accuracy, the exact magnitude of the spin density is still somewhat uncertain due to the uncertainty in the parameters that were used.[23] However, all tyrosyl radicals seem to have very similar spin density on the phenolic oxygen, with only small variations probably due to the presence or absence of a hydrogen bond. An experimental comparison of Dole et al.[54] between RNR R2 tyrosyl radical from *E. coli* and the dark stable radical in PSII yielded a small reduction of the oxygen spin density of only 0.01. For the tyrosyl radical in mouse RNR R2 a spin density of 0.34 on the phenolic oxygen was reported.[55] Compared with the more reliable values determined with isotope substitution, this value is probably incorrect. Therefore, for the hydrogen bond distance calculation in this paper we have assumed a value of 0.3 for the spin density on the phenolic oxygen of the mouse and herpes tyrosyl radical.[56] With this value we find a hydrogen bond distance of 1.89 Å for the mouse tyrosyl radical and 1.86 Å for the HSV1 tyrosyl radical. This distance is comparable to the hydrogen bond distance in the dark stable radical of photosystem II when more reliable values for the phenolic oxygen spin density are used.[52,54]

Discussion

The combined results of the Q-band ENDOR measurements and the differences in the anisotropic **g** values between the *E. coli* RNR R2 protein on one hand and the mouse and HSV1 R2 proteins on the other hand show the presence of a hydrogen-bonded tyrosyl radical in the latter two cases, which is absent in *E. coli* R2. A similar hydrogen bond to the phenolic oxygen of the tyrosyl ring has been found previously for the dark stable PSII radical.[52] Consistently in all three cases the lowering of the g_1 values is related to the presence of a hydrogen bond. This bond is responsible for the lowering of the unpaired spin density on the tyrosyl oxygen.

Hydrogen Bond Partner. The formation of the tyrosyl radical in ribonucleotide reductase is accompanied by the abstraction of a proton and an electron from the tyrosyl ring. The question remains whether the hydrogen bond measured with high-frequency EPR and pulsed ENDOR is related to this transferred proton. As previously mentioned, no crystal structures have been reported for the active, i.e., radical-containing, forms of any R2 proteins. However, the three-dimensional structures of *E. coli* apoprotein and diferrous and diferric (met)-forms of *E. coli* protein[13,57] are known as well as the structure of the mouse R2 semi-apoprotein.[14] For the *E. coli* R2 protein it was shown that the change from the apoprotein to the diferric protein was accompanied by a minor movement of the tyrosine Y122, forming the radical in combination with so-called carboxylate shifts of the iron ligands.[57,58] For the mouse RNR structures only the semi-apo protein form is known, in which only the Fe2 site furthest from the radical is occupied. This was probably due to the crystallization at pH 4.7. Therefore, some changes can be expected in the active mouse R2 protein. The structure of the HSV1 R2 is not known yet, but comparison of the amino acid sequences reveals a strong homology between mouse and HSV1 R2.[59] Since no hydrogen bond between the oxygen of the tyrosyl ring and a nearby amino acid residue could be found in neither the diferric (met) *E. coli* R2 or the mouse R2 semi-apoprotein, a likely candidate for forming a hydrogen bridge is an enclosed water molecule.

Three different water molecules in the vicinity of the tyrosyl radical have been found in the different crystal structures of the R2 protein, which we label for this discussion A, B, and C. Water A found in the crystal structure of the *E. coli* (met) R2 protein is coordinated to Fe1 in the iron−oxygen cluster and probably also present in the mouse and HSV1 R2 proteins. In the *E. coli* R2, the Y122 phenolic oxygen distance to the water A oxygen is 4.3 Å, which means that there is no hydrogen bonding possibility. In the mouse R2 semi-apoprotein structure the oxygen of water B is between the presumed Fe1 site and the tyrosyl radical (Y177) at a distance of 3.0 Å from Y177 phenolic oxygen, while water C is on the opposite side of the

(53) Hulsebosch, R. J.; van den Brink, J. S.; Nieuwenhuis, S. A. M.; Gast, P.; Raap, J.; Lugtenburg, J.; Hoff, A. J. *J. Am. Chem. Soc.* **1997**, *119*, 8685−8694.

(54) Dole, F.; Diner, B. A.; Hoganson, C. W.; Babcock, G. T.; Britt, R. D. *J. Am. Chem. Soc.* **1997**, *119*, 11540−11541.

(55) Hoganson, C. W.; Babcock, G. T. *Biochemistry* **1992**, *31*, 11874−11880.

(56) The distances derived with (pulse) ENDOR measurements depend on the oxygen spin density of the radicals. For the systems studied here this value is not precisely known and may vary somewhat between the different species, where both the distance and angle of the hydrogen bond may affect the spin density. Using eq 2 a 10% error in spin density would thus lead to a corresponding 3% error in distance r, i.e., about 0.05 Å.

(57) Aberg, A.; Nordlund, P.; Eklund, H. *Nature* **1993**, *361*, 276−278.

(58) Nordlund, P.; Eklund, H. *Curr. Opin. Struct. Biol.* **1995**, *5*, 758−766.

(59) Thelander, L.; Gräslund, A. Ribonucleotide reductase in Mammalian Systems. In *Metal Ions in Biological Systems*; Sigel, H., Sigel, A., Eds.; Marcel Dekker: New York, 1994; Vol. 30, pp 109−129.

tyrosyl plane seen from the presumed Fe1 site with a O−O distance of 2.7 Å. Waters B and C are shown in Figure 7 in Kauppi et al.[14,60] Both waters B and C are not observed in the diferric *E. coli* R2 protein structure. The ENDOR measurements cannot definitely distinguish which of these three waters is the most likely hydrogen-bonding partner. The distance between water C and the tyrosyl oxygen is 2.7 Å; thus, after subtraction of the O−D bond distance the remaining distance between the deuteron and the tyrosyl oxygen is 2.0 Å (water B) or 1.7 Å (water C). Both distances are in close agreement with the values derived from our pulsed ENDOR measurements using eq 2.

In the reported mouse R2 structure the waters B and C are placed roughly in the plane of the tyrosyl and rotated away from the C−O axis. The simulations do suggest a similar direction, but the accuracy of these simulations is limited by the poor orientation selectivity of the ENDOR measurements, even at 35 GHz.

Spin−Lattice Relaxation Effect of the Radicals. It has been shown previously that the magnetic interaction between the free radical and the iron−oxygen cluster is highly variable between different species of R2 proteins. The strongest interaction, as observed by temperature-dependent microwave saturation effects on the radical, was found for HSV1 and mouse R2, with less significant interaction in *E. coli* and *S. typhimurium* R2.[61] A more quantitative study using pulsed EPR techniques verified these results.[30] As the main source for this fast relaxation mechanism, a variation in the diferric exchange coupling was assumed. The present study shows that the difference in relaxation rate between different R2 tyrosyl radicals is correlated with the presence or absence of a hydrogen bond to the tyrosyl ring.

The exchange and dipolar (through space) components of the spin−lattice relaxation of the tyrosyl radical to the iron−oxygen cluster also depend on the distance *r* between the tyrosyl and the cluster. In the crystal structure of *E. coli* diferric R2 protein water ligands are associated with both iron ions. These waters are believed to play a role in the radical-forming reaction with molecular oxygen.[62] If this water ligand (water A) forms the hydrogen bond to the tyrosyl radical in mouse and HSV1, then the overall distance between the iron and the radical must be shorter in R2 from mouse and HSV1 compared to that in *E. coli*. Also water B is located between the cluster and the radical and might form this bridge.

Combining these considerations with the present observations, we therefore suggest an alternative explanation for the varying magnetic interaction, namely, a varying distance between the radical and the closest iron mediated by water. Two of the three closest waters are located between the cluster and the radical and are thus the most likely candidates to the mediating water. At this moment we are not able to discriminate which water is involved. The suggested hydrogen bond with an enclosed water molecule is in contrast to $Y_D^{\bullet}$ from PSII where it was shown recently[50] that the hydrogen donor is a nearby histidine (His189).

Radical Stability. In the study by Kauppi et al.[14] a comparison was made between the structures of ribonucleotide reductase from *E. coli* and mouse. It was concluded that the active site of mouse RNR R2 is more accessible to solvent compared to that of RNR R2 from *E. coli*. This includes a hydrophobic channel that is blocked by a tyrosine (Tyr 209) in the *E. coli* R2 protein. Exchange studies of the oxygen in the diiron−oxygen cluster showed, however, that the site in RNR from *E. coli* was also accessible for solvent molecules.[62] The overall effect of the difference in structure is a less stable environment of the active site in the mouse and HSV1 R2 protein compared to RNR from *E. coli* and *S. typhimurium*. The stabilizing influence of the hydrogen bridge by delocalizing the spin density of the phenolic oxygen may help to provide the extra stability needed for the more accessible (i.e., mouse and HSV1 R2) tyrosyl radicals.

Acknowledgment. P.J.v.D. thanks the EPR group at Northwestern University for their hospitality during his stay there. The help of Mr. Adri A. K. Klaassen and Mr. Clark E. Davoust with the measurements is greatly acknowledged. We thank the staff of the Nijmegen High-Field Magnet Laboratory for the use of their Bitter magnet in the high-frequency EPR experiments. This research was supported by The Netherlands Organization for Chemical Research (SON) with financial aid from the Foundation for Scientific Research in The Netherlands (NWO), NIH Grant HL13531 and RR11721 (to B.M.H.), the Swedish Natural Science Research Council (to A.G.), and the Research Council of Norway (to K.K.A.). The high-frequency EPR spectrometer (130 GHz) is part of an EC project for the development of an ultra-high-field biological electron spin resonance large-scale facility (UMBELLA) under TMR Project No. ERBFMGECT-950008. The high-frequency experiments at Grenoble were made possible by support from TMR Project No. ERBFMGECT950077. P.P.S. was supported by a Marie Curie Training Grant, TMR-ERB4001GT962965, and S.P. by a fellowship from the Deutscher Akademischer Austauschdienst. Traveling grants from the Nordic EPR network are greatly acknowledged.

JA9737127

(60) The two waters can be found in pdb data file 1XSM.pdb as atoms 2396 (B) and 2397 (C).

(61) Sahlin, M.; Petersson, L.; Gräslund, A.; Ehrenberg, A.; Sjöberg, B.-M.; Thelander, L. *Biochemistry* **1987**, *26*, 5541−5548.

(62) Ling, J.; Sahlin, M.; Sjöberg, B.-M.; Loehr, T. M.; Sanders-Loehr, J. *J. Biol. Chem.* **1994**, *269*, 5595−5601.